J. Am. Ceram. Soc., 95 [12] 3763–3768 (2012)
DOI: 10.1111/j.1551-2916.2012.05444.x

journal

Porous Ceramics by Photopolymerization with Terpene–Acrylate Vehicles

Vladislava Tomeckova and John W. Halloran†

Department of Materials Science and Engineering, University of Michigan, Ann Arbor, Michigan 48109

A novel terpene–acrylate photopolymerizable vehicle was used to fabricate porous polymer-ceramic composites and sintered porous ceramics. The vehicle consists of camphene, camphor and a diacrylate monomer. Alumina or silica suspensions were mixed above the melting point of the terpene. Upon cooling, the terpene crystallized from the solution as particle-free dendrites, with the powder and liquid monomer in the interdendritic spaces. The monomer could subsequently be solidified by photopolymerization. The rheological behavior is reported for ceramic suspensions in the molten terpene–monomer solution. The photopolymerization cure depth versus energy dose is reported for silica and alumina systems. The microstructure of the porous solid is characterized for systems with camphor/camphene and menthol as terpene. The structure of the dendritic porosity is compared as a function of powder volume fraction, for particles smaller or larger than the dendrite arm spacing.

I. Introduction

Freeze casting is widely used for porous materials[1,2] using water ice or vehicles such as terpenes[3] or other convenient suspension vehicles that can be frozen. If the ceramic volume fraction is sufficiently low, ice templating occurs[4] where the growing ice crystals redistribute the particles[5] to create pore-free regions as lamellae,[6] dendrites, or spherulites.[7] Typically, the pore-forming crystals are removed by sublimation. Sublimation of water ice is done by cryogenic freeze drying. More volatile solids, such as the terpene camphene, can be removed by sublimation at room temperature. Camphene and other terpenes offer the convenient property of room temperature freeze casting, where warm (~80°C) liquid suspensions crystallize below around 50°C, so can be cast at room temperature.

At times it may be more convenient to polymerize the ceramic green body, so that materials surrounding the ice templates are permanently solidified by curing. If the matrix is cured, the ice templates can simply be melted away, avoiding the inconvenience of sublimation. This use of photopolymerization with freeze templating was demonstrated recently for a variety of microshapes and multilayers using photopolymerization of water-based systems.[8] Photopolymerization enables patterning. Patterned layers can be used as single layers, or many layers can be combined to produce large complex-shaped ceramics by stereolithography[9] and other methods.[10] Photopolymerization is also effective for microshaping.[11] Thick films of photopatterned porous ceramics could be used as single layers, or many layers could be laminated to make 3D objects. In this case the photopatterned designs remain as solid, while the unexposed material can be removed by remelting to liberate the 3D design. Photopatterned laminates would enable a freeform fabrication method for ceramics that is a hybrid of the photopolymerizable liquid-based methods and the solid tape lamination methods.[12]

This study presents a novel system that combines room temperature freeze casting to produce ice-templated frozen solid layers, which can be subsequently patterned by photopolymerization to selectively cure the frozen layers. The photocured regions are permanently solidified, but the uncured regions can be melted away. Figure 1 shows the scheme of the preparation procedure. The vehicle consists of a mixture of acrylate monomers (which can be polymerized) and terpenes which are liquid when warm, but are crystalline at room temperature. Certain compositions of terpene–acrylate mixtures[13] are fluid single-phase solutions at 100°C, and two-phase soft solid systems at room temperature. The room temperature solid consists of crystalline dendrites of the terpenes, with the acrylate monomer as an interdendritic liquid. We have shown that the interdendritic monomer can be photopolymerized to solid polyacrylate. Removing the terpene dendrites by melting or sublimation produces ice-templated porous plastic films.[13] Here we use the terpene–acrylate mixture as the suspension medium for ceramic powders, and use the freeze casting/photopolymerization method for ice-templated porous ceramic layers. This process is demonstrated for a silicon dioxide and alumina ceramic.

II. Experimental Procedure

(1) Materials

Three terpenes were explored—menthol, camphor, and camphene. These are nontoxic aromatic substances derived from plants. Some physical properties of the terpenes[7,14,15] are shown in Table I. The (±)-Camphene, 97% and DL-camphor, 96% were used as-received from the supplier (Alfa Aesar/Avocado Organics, Ward Hill, MA). Camphene exhibits soft crystallinity at room temperature. The camphor (DL-camphor or DL-2-Bornanone) occurs in the form of white crystalline particles. Both camphor and camphene have the characteristic aroma of incense. The menthol was L-menthol, 99% (Alfa Aesar) which is (1R,2S,5R)-2-Isopropyl-5-methylcyclohexanol. Menthol occurs in the form of white crystalline needles. The crystals have the familiar smell of menthol, which is quite strong when it is melted.

The thermoreversible photocurable vehicle is a composition of terpenes and an acrylate monomer. The range of compositions of monomers with terpenes which are liquid at 100°C and sufficiently rigid at 25°C has been reported elsewhere.[13] These terpenes are polar substances, and work well with water-dispersible monomers such as polyethylene glycol (400) diacrylate (SR344; Sartomer Co., Exton, PA). Polyethylene glycol (400) diacrylate is a bifunctional acrylate monomer that produces soft flexible films upon polymerization. As presented in detail elsewhere,[13] a vehicle consisting of 40 wt % diacrylate, 40 wt% camphene, and 20 wt% camphor was a clear single phase liquid solution above 50°C. Below 40°C, the camphene/camphor portion is completely frozen, with the diacrylate monomer (and suspended powder) as an interdendritic liquid. At this temperature, the vehicle is a soft solid that can be handled like a ceramic green tape.

L. Gauckler—contributing editor

Manuscript No. 31327. Received April 13, 2012; approved August 13, 2012.
†Author to whom correspondence should be addressed. e-mail: peterjon@umich.edu

Two refractory-grade milled fused silica powders were used as received. The coarser powder (CE44CSS; CE Minerals, particle size d_{10} = 2 μm, d_{50} = 8.5 μm, and d_{90} = 36.8 μm) had median particles which were significantly larger than the typical secondary dendrite arm spacing for camphene. The finer fused silica powder (TECOSIL-10, particle size d_{50} = 4 μm, d_{90} = 14 μm), had a median particle size smaller than camphene dendrite arm spacing. The density of silica powders is 2.2 g/cm^3. The alumina powder (A16-SG; Alcoa Inc., Pittsburgh, PA) has particles with diameter 0.4 μm, relatively narrow size distribution, surface area 8.6 m^2/g and density 3.92 g/cm^3 (all from the manufacturer's specification). The colloidal dispersant for the ceramic suspensions was Variquat CC-59 (Evonik Goldschmidt Corporation, Hopewell, VA), which is diethyl polypropoxy-2 hydroxyethyl ammonium phosphate (1.04 g/cm^3) with pH varying from 7.5 to 9 (all according to the manufacturer's specifications). Variquat CC-59 was added at 3 wt% with respect to the weight of the ceramic powder. To render the ceramic suspensions in terpene –diacrylate monomers photoopolymerizatible, we added 2% with respect to monomer mass of a commercial ketone photoinitiator 1-hydroxy-cyclohexyl-phenyl-ketone (Irgacure 184; Ciba Specialty Chemicals, Tarrytown, NY).

(2) Fabrication Procedure

Ceramic suspensions were prepared by warm ball milling. Suspensions were sealed in a polyethylene jar to prevent the loss of the volatile vehicle and ball milled at the speed of ~30 rpm at about 100°C, using a small roller mill installed inside a warm oven. The terpene–monomer, with the dispersant was heated to 100°C. When the vehicle was fully melted, the ceramic powder was added and ball milled for 1 h at 100°C. The photoinitiator was added and the systems were ball milled for an additional 30 min. This final milling was done at 75°C to avoid thermopolymerization as most of the photoinitiators are thermoinitiators above ~80°C. The as-prepared suspensions could be frozen and remelted with no apparent degradation.

The warm ceramic suspensions were poured into aluminum foil weighing dishes (1 cm height, ~4 cm diameter) and left to freeze at room temperature. The material was photopolymerized at room temperature shortly after solidification.

(3) Characterization

Ceramic suspensions in molten camphene/camphor/PEG (400) diacrylate liquids are unusual, so we characterized the flow behavior using a rheometer (AR1000; TA Instruments, New Castle, DE) with cone and plate geometry (4 cm diameter, 1.59°C, trunctuation 44 μm). The temperature is controlled to within ±1°C and a solvent trap minimized the evaporation during the experiment. The shear rate dependence of the viscosity was measured from 0.5 to 100 s^{-1} at a constant temperature of 75°C. The effect of temperature was measured from 50°C to 80°C for viscosity at a constant shear rate of 45 s^{-1}.

The photopolymerization behavior was characterized by measuring the depth of cured layers C_d as a function of UV energy dose, E. The experiments with the silica suspensions were performed in a UV lamp chamber (Postcure unit (PCU) apparatus; 3D Systems Inc., Valencia, CA) illuminated with UV fluorescent lamps Philips (Philips Electronics North America Corporation, Andover, MA) TLK 40W/05 emitting light in the wavelength range 320–480 nm (with 360 nm strong peak) and intensity ~2 mW/cm^2. Samples frozen at room temperature were covered with a UV-opaque mask with two UV transparent windows (1 cm × 1.5 cm). The samples were exposed to energy doses ranging from 60 to 250 mJ/cm^2. This energy dose was sufficient to produce polymerized samples with thickness on the order of 1–2 mm for the silica-filled system. After polymerization, the aluminum foil dishes were placed in an oven at 75°C, where the uncured material was melted away while the polymerized windows remained solid. Polymerized windows recovered from the re-melted suspensions were gently rinsed with isopropanol. The cure depth C_d was the thickness as measured with a micrometer. The cure depths C_d were plotted against the logarithm of the energy dose E, which gives a linear function of the form $C_d = D_p \ln (E/E_c)$. The slope reports the sensitivity D_p and the critical energy dose E_c is evaluated from the energy dose intercept.

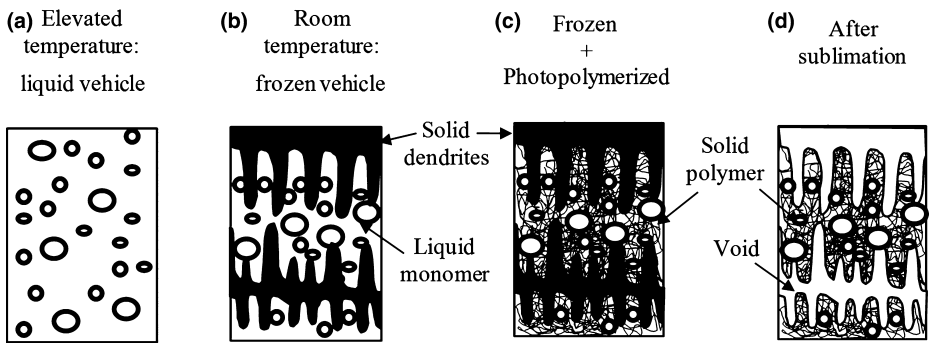

Fig. 1. Scheme of the preparation of porous polymers with dendritic shaped interconnected porosity. From left: (a) Above terpene melting point, a suspension of ceramic powder in a liquid solution of terpene and liquid monomer; (b) After solidification of the terpene: Partially frozen solid with ceramic-free terpene dendrites and liquid suspension of ceramic powder in monomer in the interdendritic spaces; (c) After photopolymerization of monomer: Solid ceramic-filled polymer in the shape of the interdendritic spaces with solid terpene dendrites; (d) After sublimation (or melting away) of terpenes: Solid ceramic-filled polymer with voids in the shape of the former terpene dendrites. Subsequent heating burns off the polymer and sinters the ceramic.

Table I. Some Physical Properties of Camphene, Camphor, and Menthol

	Chemical formula	Melting point (°C)	Density at 20°C (g/cm^3)	Liquid viscosity (mPa s)	Vapor pressure in solids (Pa)
Camphene	$C_{10}H_{16}$	44–48	0.85	1.4 (47°C)	2×10^3 (55°C)
Camphor	$C_{10}H_{16}O$	173–175	0.992	0.63 (180°C)	1.3×10^2 (41°C)
Menthol	$C_{10}H_{20}O$	43–45	0.89	–	1.3×10^2 (56°C)

D_p and E_c were determined for alumina compositions with a different procedure. The experiments were conducted in a stereolithography apparatus (SLA-250), using a solid state laser (Xcyte; JDSU, Milpitas, CA) that had a quasi-continuous wave emitting at 355 nm, output power 30 mW, and a beam diameter of 125 μm. The intensity of the laser beam was measured before each experiment using a built-in sensor which had been calibrated with a thermal laser power meter (Orion-TH; Ophir Optronics, Jerusalem, Israel). The subsequent process of melting away the uncured material, cleaning with isopropanol, and measurements with micrometer were the same as in the case of the silica compositions.

The silica specimens for the microstructure analysis were polymerized in the UV lamp chamber at ~450 mJ/cm^2 and had thickness of several millimeters. The alumina specimens were polymerized using a dose of ~3000 mJ/cm^2 in stereolithography apparatus and cured only to a depth of a few hundreds of micrometers. Uncured material was melted away in an oven at 75°C and the samples were gently rinsed with isopropanol. The microstructure of fracture surfaces of the ceramic-filled polyacrylates was investigated using secondary electron imaging in a scanning electron microscope.

The silica-filled polyacrylates underwent the process of binder burnout at 600°C and sintering at 1300°C for 30 min (heating ramp 3°C/min, cooling ramp 5°C/min–300°C and 1°C/min–25°C). Apparent porosity and relative density of sintered bodies was determined via the Archimedes water displacement method. SEM was used to observe the microstructure of the sintered ceramic bodies.

III. Results and Discussion

(1) Rheology of Warm Liquid Suspensions

The diacrylate/camphene/camphor vehicle is a Newtonian liquid at 75°C with a viscosity of about 0.003 Pa s. The viscosity versus shear rate at 75°C for suspensions with finer silica, and alumina (3, 15, 25, and 35 vol%) are shown in Fig. 2. Experiments were conducted in the shear rate range of 0.5–100 s^{-1}. The silica suspensions were nearly Newtonian while the alumina suspensions are slightly shear thinning. The shear thinning effect diminishes at smaller ceramic solid loading. The suspensions were approximately Newtonian at a shear rate of 45 s^{-1}, and the apparent viscosity was measured as a function of temperature in the temperature range 50°C–80°C.

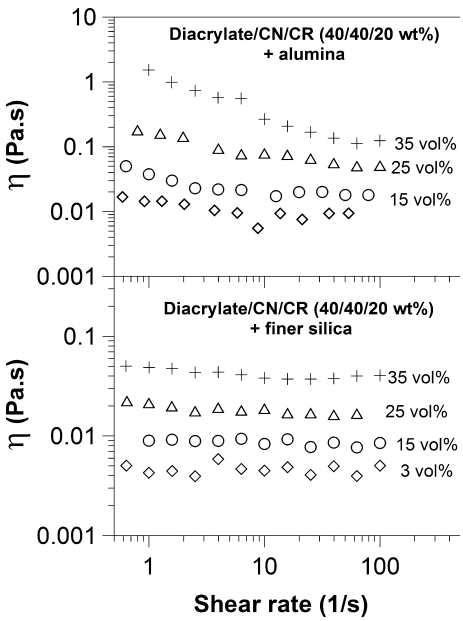

Fig. 2. Apparent viscosity versus shear rate for terpene–acrylate suspensions filled with alumina and finer silica. Experiments were conducted at 75°C.

These data are shown in Fig. 3. The viscosity data could be satisfactorily fit with the Arrhenius plot and the apparent activation energy, summarized in Table II, seems to decrease with solid loading. However, upon closer examination, the temperature dependence of the viscosity is the same for all suspensions. This can be seen in the top part of Fig. 3, which shows the viscosity data for all suspensions normalized by the 60°C viscosity. All the data points overlap, suggesting that the temperature dependence is the same for all suspensions, with an apparent activation energy of 18.1 ± 0.1 kJ/mol.

(2) Photopolymerization Behavior

The penetration depth D_p and critical energy dose E_c are reported in Table III as a function of the ceramic volume content for the alumina and the finer silica powders. Penetration depth D_p of silica suspensions fluctuates around ~950 ± 150 μm for all compositions, which is similar to the unfilled vehicle (D_p = 950 μm). On the other hand, the alumina-filled system had a much smaller penetration depth even at small solid loadings (3 vol%). The composition with

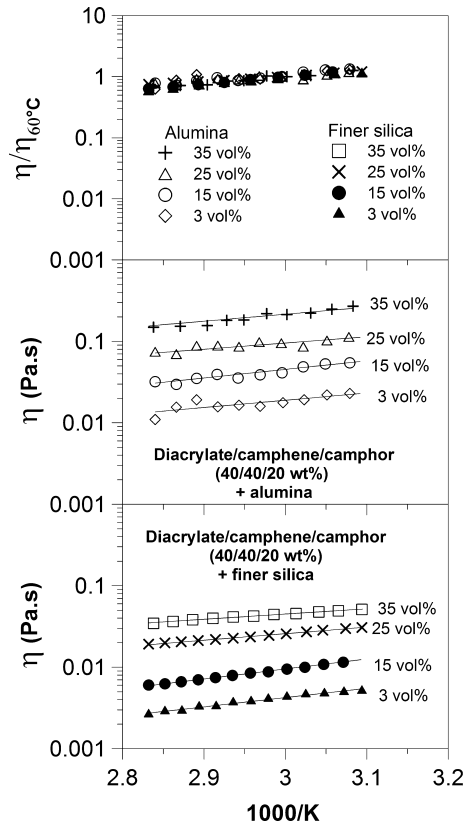

Fig. 3. Viscosity at 45 s^{-1} versus temperature. Bottom: finer silica powder at four solid loadings; Center: alumina powder at four solid loading; Top: viscosity relative to viscosity at 60°C for both powders at four solid loadings.

Table II. Apparent Activation Energies for Viscosity for Suspensions with Alumina and the Finer Silica Powder in Diacrylate/Camphene/Camphor (40/40/20 wt%) at 45 s^{-1}

	Activation energy (kJ/mol)	
Ceramic volume fraction (Φ)	Alumina powder	Finer silica powder
0.03	17.1 ± 1.4	23.4 ± 0.2
0.15	20.2 ± 1.8	22.5 ± 0.2
0.25	14.7 ± 0.6	14.7 ± 0.1
0.35	16.5 ± 0.9	13.1 ± 0.1

Table III. Variation of Photopolymerization Dose Parameters with Ceramic Volume Fraction, Showing Sensitivity D_p and Critical Energy E_c for the Alumina Powder and Finer Silica Powder

Ceramic volume fraction	Alumina				Finer silica			
	D_p (μm)	$E_{c\ average}$ (mJ/cm^2)	$E_{c\ min}$ (mJ/cm^2)	$E_{c\ max}$ (mJ/cm^2)	D_p (μm)	$E_{c\ average}$ (mJ/cm^2)	$E_{c\ min}$ (mJ/cm^2)	$E_{c\ max}$ (mJ/cm^2)
0	950 ± 170	49	28	85	950 ± 170	49	28	85
0.03	353 ± 44	50	25	97	900 ± 135	39	27	58
0.15	129 ± 14	21	10	44	947 ± 150	28	10	55
0.25	125 ± 8	38	26	57	871 ± 134	19	11	32
0.35	108 ± 23	32	11	85	950 ± 70	20	15	26

35 vol% alumina has D_p of ~100 μm, which is ~10 times smaller than in silica compositions. Reduced penetration depth decrease was observed previously also in other alumina-filled photosuspensions.[16]

The average critical energy dose E_c decreases from ~50 to 20 mJ/cm^2 for the silica suspensions with 0–35 vol%, respectively. Similarly, the E_c of alumina suspensions decreases from ~50 to 30 mJ/cm^2 for the alumina compositions. Note that the E_c values are obtained by extrapolation from a regression line from a semi-log plot of cure depths versus energy dose. The standard errors for both ln E_c and D_p were estimated from the residual sum of squares, using a statistical analysis package (OriginPro 8; OriginLab Corporation, North Hampton, MA). The standard error in ln E_c corresponds to a minimum and maximum in the E_c value.

(3) Microstructures of Porous Materials

(A) Ceramic-Filled Polyacrylates Before Binder Burnout and Sintering: These materials are similar to conventional freeze-cast ceramics, featuring interconnected pore channels, about 5 μm wide, created by the growth of camphene dendrites, which redistribute the ceramic and acrylate liquid to the interdendritic spaces. The size of the ceramic particles is in the same range as the cross-section of the camphene dendrites. The alumina suspension has particles much smaller than the size of dendrites, while the finer silica has particles comparable with the size of the dendrites, and the coarser silica has particles larger than the dendritic structures.

After removal of the terpene, and before binder burnout, the materials are porous cellular composites with ceramic-filled polyacrylate cell walls. The polyacrylate with ceramic forms the cell walls while the voids are the replicas of terpene dendrites. The macropores are smaller when the solid loading is higher. This is shown in Fig. 4 for the alumina–acrylate system. At low solid loading, the dendrites are quite well formed and regular, but at higher solid loading, the macroporosity is irregular. The shape of the pores depends upon the ceramic volume content and the solidification conditions. For the low ceramic volume content (3 vol%) the pores are uniform and grow in one direction. Dendritic formation in compositions with higher ceramic loadings (35 vol%) was more disrupted and unidirectional colonies of terpene dendrites formed. Thicker polyacrylate/ceramic walls were also observed in compositions with higher ceramic loadings where less terpenes are present to form a dendritic network.

The macropore size, estimated by measuring the side dendrite spacing and subtracting the cell was thickness, is smaller for higher solid loading. These values are reported in Table IV. The influence of particle size appears in Fig. 5, which compares the fracture surface for the 3 vol% silica–polyacrylate for both the finer silica and the coarser silica. The microstructures are roughly comparable for these dilute suspensions. At the 35 vol% loading the less-regular dendritic structure occurs with both silica powders. Large particles are visibly embedded within the dendritic structure for the coarse powder (d_{90} = 36.8 μm). This is shown more clearly in Fig. 6, which shows a grown dendrite around the larger particles.

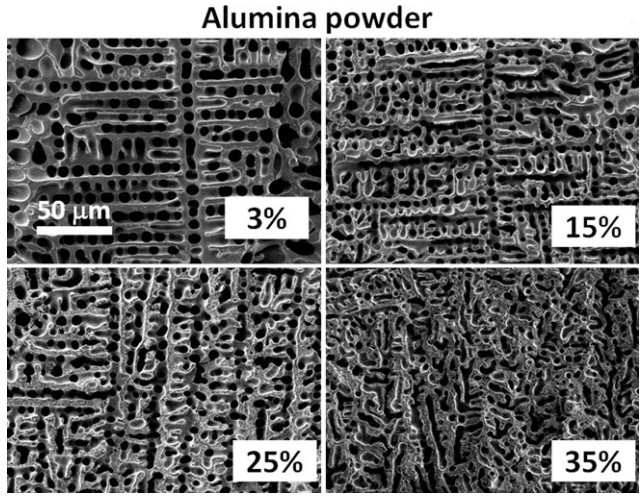

Fig. 4. Fracture surface of alumina-filled polyacrylates showing influence of solid loading on dendritic pore morphology.

Changes in the ceramic/monomer/terpene composition will change the composition of the macroporous composite after removal of the terpene dendrites. The fraction of macroporosity varies with the terpene volume fraction. The ceramic/polymer ratio in the porous-filled polyacrylate varies with the ceramic/monomer ratio, and the macropore size varies with the ceramic volume fraction. This appears in Table IV, summarizing the four solid loading for the three powders.

(B) Porous Ceramics After Sintering: Menthol-diacrylates were explored as an alternative vehicle. The morphology of menthol crystallized from solution is spherulitic,[13] as opposed to the branched dendrites of camphor/camphene. A series of compositions with a diacrylate/menthol (40/60 wt%) vehicle was used with the finer silica at powder loadings of 15, 25, and 35 vol%. The process of preparation was the same as for the compositions based on diacrylate/camphene/camphor. After polymerization, the menthol melted and evaporated during binder removal thermal treatment (up to 600°C) and this was followed by sintering at 1300°C for 30 min.

Figure 7 compares the fracture surfaces of the sintered silica ceramics with 15 vol% finer silica. Figure 7(a) had a diacrylate/camphene/camphor (40/40/20 wt%) vehicle and Fig. 7(b) had a diacrylate/menthol vehicle. The pores are replicas of the voids after terpene sublimation. The dendritic shape is for compositions with camphene/camphor, while spherulitic shape porosity occurs in compositions with menthol, as the crystallization of menthol in this system is spherulitic. The cell walls are bonded microporous silica. As these are refractory silicas, incomplete densification is expected at 1300°C. The relative density and apparent porosity of the sintered bodies are presented in Table V. The apparent porosity was ~73%, 64%, and 55% for systems containing 15, 25, and 35 vol% ceramics, respectively. The apparent porosity was about the same for compositions with finer and coarser silica and for compositions containing menthol in the

Table IV. Composition of the Original Suspensions (Prior Polymerization) and Composition of Polymerized Polyacrylate Filled with Ceramics after Terpene Sublimation. The thermoreversible polymerizable vehicle was diacrylate/camphene/camphor (40/40/20 wt%)

Suspension composition			Polymerized material composition (after terpene sublimation)		Macropore size (μm)		
$\Phi_{ceramic}$ (vol%)	$\Phi_{monomer}$ (vol%)	$\Phi_{terpenes}$ (vol%)	$\Phi_{ceramic}$ (vol%)	$\Phi_{polymer}$ (vol%)	Alumina	Finer silica	Coarser silica
3	33.0	63.2	9	91	7.1 ± 1.4	7.3 ± 1.0	6.3 ± 0.6
15	28.7	54.9	37	63	4.8 ± 1.1	5.3 ± 1.1	5.3 ± 1.0
25	25.0	48.0	53	47	5.4 ± 1.0	4.2 ± 0.3	4.2 ± 0.9
35	21.4	41.1	65	35	3.0 ± 0.7	3.0 ± 0.6	3.4 ± 0.8

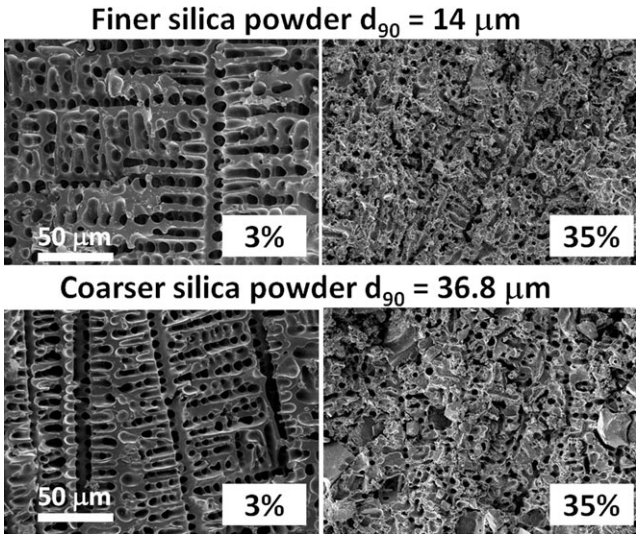

Fig. 5. Fracture surface of silica-filled polyacrylate, showing influence of silica particle size for the finer d_{90} = 14 μm and coarser d_{90} = 36.8 μm for dilute suspensions (3%) and concentrated suspensions (35%).

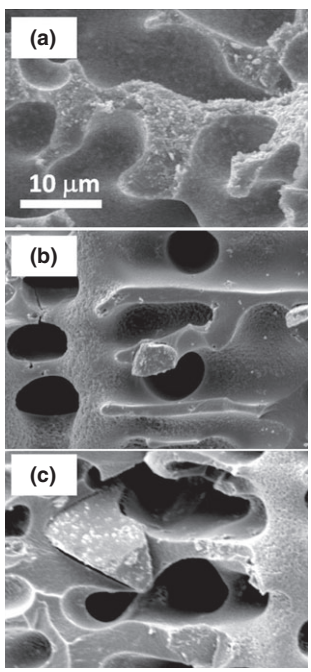

Fig. 6. Detail of fracture surfaces of ceramic-filled polyacrylate after removal of terpenes. The vehicle was diacrylate/camphene/camphor 40/40/20 wt%. (a) 25 vol% alumina; (b) 3 vol% finer silica; (c) 3 vol% coarser silica.

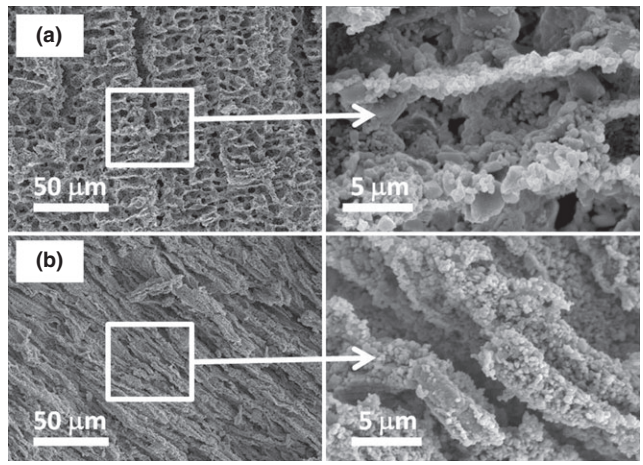

Fig. 7. Comparison of sintered ceramics prepared with 15 vol% of the finer silica powder. (a) Dendritic macropores with diacrylate/camphene/camphor (40/40/20 wt%) vehicle; (b) Spherulitic macropores with diacrylate/menthol (40/60 wt%) vehicle.

Table V. Sintered Density and Apparent Porosity of Silica Porous Ceramics

Thermoreversible photopolymerizable vehicle	Ceramic	Ceramic volume fraction (Φ)	Dry bulk density (g/cm^3)	Apparent porosity (vol%)
Diacrylate/CN/CR (40/40/20 wt%)	Coarser silica	0.15	0.66	70
		0.25	0.83	64
		0.35	1.02	55
Diacrylate/CN/CR (40/40/20 wt%)	Finer silica	0.15	0.60	73
		0.25	0.79	64
		0.35	1.00	54
Diacrylate/menthol (40/60 wt%)	Finer silica	0.15	0.62	74
		0.25	0.82	63
		0.35	1.02	54

original suspension. Note that the polyacrylate removal during binder burnout results in about 15% higher porosity in the sintered ceramics when compared with ceramic-filled polyacrylates (Table IV).

IV. Discussion

The fabrication method presented here combines the freeze casting ice-templating method with photopolymerization. Freezing of the terpenes converts the suspension into a soft solid, which can be re-liquefied by melting. Photopolymeriza-

tion causes an irreversible solidification, so the cured areas remain solid when the noncured areas are melted. This technique presents some new opportunities in ceramic forming. This system could be used for casting tapes which can be patterned by photopolymerization. This may provide a method to fabricate complex shaped 3D objects with ice templated porosity (here "ice" means any frozen substance).

The limited cure depth for photopolymerization restricts this method to films no thicker than the cure depth, which is often on the order of a millimeter. However, bulk ceramics could be produced from these systems by replacing the substituting conventional thermal polymerization for surface-sensitive photopolymerization, as a type of ice-templated gel casting. The bulk thermal polymerization would have to occur at temperatures below the terpene melting point. For acrylate gel casting, thermal initiation can be done around room temperature by accelerating the decomposition of the standard benzoyl peroxide initiator with a suitable catalyst, such as *n,n* dimethyl-*p*-toluidine.[17] This would enable the fabrication of bulk ice-templated shapes. Of course, ordinary freeze casting already enables bulk ice-templated shapes. However, it is difficult to freeze dry large objects, as heat and mass transfer required to sublime the ice become slow with larger objects. Moreover, the size of the dendrites necessarily scales with the solidification rate,[5,6] which is fast near the surface and slow in the interior. This creates nonuniform ice-template pores, smaller near the surface and larger in the interior. A large shape with uniform ice-template pores could be made by laminating thin tapes, each with the same solidification rate. Or a large object with tailored pores could be made by combining tapes frozen with different solidification rates, and having different pore size.

Nonporous objects could also be produced. At the low ceramic loadings presented here, the terpene dendrites create pore channels. However, dendritic porosity does not produce sufficiently high ceramic loadings,[18] so dense patterned ceramics could also be produced with these media.

V. Conclusion

Ceramic-filled polyacrylates with up to ~63 vol% porosity and sintered porous ceramics with up to ~72 vol% porosity were prepared using a thermoreversible photopolymerizable vehicle consisting of terpenes and a diacrylate monomer. Above the melting point of the terpenes, the powder suspensions form fluid dispersions in the liquid solution of terpenes in diacrylate. The variation of the viscosity with temperature can be described with an apparent activation energy which decreases with ceramic powder volume fraction.

The melting point of the vehicle is slightly above the room temperature, which enables easy preparation of the liquid compositions followed by solidification at room temperature, when the terpenes crystallize. As the terpene solidification front proceeds, the ceramic particles and the monomer are expelled in the interdendritic space. The ceramic–monomer liquid in the interdendritic space can be photopolymerized. The photopolymerization dose parameters vary with the type and amount of ceramic. Subsequent sublimation of the terpenes leaves a porous solid with ceramic-filled polyacrylate walls with continuous pore channels about 5 μm wide, reflecting the dendritic network of the terpenes. Interconnected dendritic macropore channels were achieved in systems with camphene/camphor and spherulitic macropore channels in systems with menthol in the original composition. The width of the macropore channels decreases with ceramic volume fraction.

Acknowledgments

This research was supported by the United States Defense Advanced Research Projects Agency (DARPA) under HR0011-07-1-0034, Program Officer W. S. Coblenz and the Office of Naval Research under N00421-06-1-002, Program Officer David Shifler

References

[1]S. Deville, E. Saiz, R. K. Nalla, and A. P. Tomsia, "Freezing as a Path to Build Complex Composites," *Science*, **311**, 515–8 (2006).
[2]E. Munch, E. Saiz, A. P. Tomsia, and S. Deville, "Architectural Control of Free-Cast Ceramics Through Additives and Templating," *J. Am. Ceram. Soc.*, **92** [7] 1534–9 (2009).
[3]K. Araki and J. W. Halloran, "Porous Ceramic Bodies with Interconnected Pore Channels by a Novel Freeze Casting Technique," *J. Am. Ceram. Soc.*, **88** [5] 1108–14 (2005).
[4]S. Deville, E. Saiz, and A. P. Tomsia, "Ice-Templated Porous Alumina Structures," *Acta Mater.*, **55**, 1965–74 (2007).
[5]N. O. Shanti, K. Araki, and J. W. Halloran, "Particle Redistribution During Dendritic Solidification of Particle Suspensions," *J. Am. Ceram. Soc.*, **89** [8] 2444–7 (2006).
[6]T. Waschkies, R. Oberaker, and M. J. Hoffmann, "Control of Lamellae Spacing During Freeze Casting of Ceramics Using Double-Side Cooling as a Novel Processing Route," *J. Am. Ceram. Soc.*, **92**, S79–84 (2009).
[7]K. Araki and J. W. Halloran, "Room-Temperature Freeze Casting for Ceramics with Nonaqueous Sublimable Vehicles in the Naphthalene-Camphor Eutectic System," *J. Am. Ceram. Soc.*, **87** [11] 2014–9 (2004).
[8]Y. de Hazen, "Porous Ceramics, Ceramic/Polymer, and Metal-Doped Ceramic/Polymer Nanocomposites via Freeze Casting of Photo-Curable Colloidal Fluids," *J. Am. Ceram. Soc.*, **95** [1] 177–81 (2012).
[9]F. Doreau, C. Chaput, and T. Chartier, "Stereolithography for Manufacturing Ceramic Parts," *Adv. Eng. Mater.*, **2** [8] 493–6 (2000).
[10]J. W. Halloran, V. Tomeckova, S. P. Gentry, S. Das, P. Cilino, D. Yuan, R. Guo, A. Rudraraju, T. Wu, W. Baker, D. Legdzina, D. Wolski, W. Zimbeck, and D. Long, "Photopolymerization of Powder Suspensions for Shaping Ceramics," *J. Eur. Ceram. Soc.*, **31**, 2613–9 (2011).
[11]Y. de Hazen, M. Wozniak, J. Heinecke, G. Muller, and T. Graule, "New Microshaping Concepts for Ceramic/Polymer Nanocomposites and Nanoceramic Fibers," *J. Am. Ceram. Soc.*, **93**, 2456–9 (2010).
[12]R. H. Evans, "Seventy Ways to Make Ceramics," *J. Eur. Ceram. Soc.*, **28**, 1421–32 (2008).
[13]V. Tomeckova and J. W. Halloran, "Highly Porous Polymers via a Novel Terpene-Acrylate Thermoreversible Photopolymerization Vehicle," *J. Mater. Sci.*, **47**, 6166–78 (2012).
[14]T. E. Daubert and R. P. Danner, *Physical and Thermodynamic Properties of Pure Chemicals: Data Compilation, Part 4*. Taylor & Francis, London, UK, 1989.
[15]D. R. Stull, "Vapor Pressure of Pure Substances Organic Compounds," *Industr. Eng. Chem.*, **39**, 517–40 (1947).
[16]V. Tomeckova and J. W. Halloran, "Cure Depth for Photopolymerization of Ceramic Suspensions," *J. Eur. Ceram. Soc.*, **30**, 3023–33 (2010).
[17]C. Reilly, W. Chappell, J. W. Halloran, and L. P. B. Katehi, "High Frequency Electromagnetic Bandgap Structures via Indirect Solid Freeform Fabrication," *J. Am. Ceram. Soc.*, **87** [8] 1446–53 (2004).
[18]K. Araki and J. W. Halloran, "New Freeze-Casting Technique for Ceramics with Sublimable Vehicles," *J. Am. Ceram. Soc.*, **87** [10] 1859–63 (2004). □